Volume 2023, 15 pages | Article ID : IJPGE-2212052112830

International Journal of Petroleum and Geoscience Engineering

Journal homepage: www.htpub.org/ijpge/

ISSN: 2289-4713

# Artificial Neural Network (ANN) Prediction of Porosity and Permeability of Shaly Gas Sandstone Reservoir using NMR Data

Ghareb Mostafa Hamada [a,*], Mahmoud Abushanab [b]

[a]*Petroleum Engineering Department, College of Engineering, The American University of Kurdistan, Kurdistan, Iraq*
[b]*Shell Egypt, Egypt*

**Article**

Article history
Received: 12 October 2022
Received in revised form: 15 November 2022
Accepted: 06 December 2022

Keywords:
Neural network,
Porosity,
Permeability,
NMR,
Conventional logs and shale gas sand reservoirs

**Abstract**

Petrophysical evaluation of shaly gas sand reservoirs is one of the most difficult problems. These reservoirs usually produce from multiple layers with different permeability and complex formation, which is often enhanced by natural fracturing. In this study, we propose a new model to predict porosity and permeability using derived data from NMR. The developed Artificial Neural Network (ANN) model uses the NMR T2 pin values, density and resistivity logs to predict porosity, and permeability for two test wells. The NN trained model has displayed good correlation with core porosity and permeability values, and with the NMR derived porosity and permeability in the test wells. This work focuses on determination of porosity ($\varphi_{DMR}$) from combination of density porosity, NMR porosity and permeability from NMR logs using Bulk Gas Magnetic Resonance Permeability (KBGMR). Neural network (ANN) technique is used to predict formation porosity and permeability using NMR and conventional logging data. Predicted porosity and permeability have shown a good correlation about 0.912 with core porosity and about 0.891 for permeability in the studied shaly gas sand reservoir.

## 1. Introduction

Porosity logs measurements require environmental corrections and are influenced by lithology and formation fluids. The porosity derived is the total porosity, which consists of producible fluids, capillary bound water and clay-bound water. However, NMR provides lithology independent porosity and includes only producible fluids and capillary bound water. Permeability is a measure of fluid rock conductivity. To be permeable, a rock must have interconnected porosity. Greater porosity usually corresponds to greater permeability; however, this is not always the case. Formation permeability is influenced by pore size, shape and continuity, as well as the amount of porosity. Permeability can be determined from resistivity gradients, permeability models based on porosity, φ, and irreducible water saturation (Swi), formation tester (FT) and nuclear magnetic resonance (NMR). Perhaps, the most important feature of NMR logging is the ability to record a real-time permeability log. The potential

*Corresponding author at: Petroleum Engineering Department, College of Engineering, The American University of Kurdistan, Kurdistan, Iraq
Email address: ghareb.hamada@auk.edu.krd

benefits of NMR to oil companies are enormous. Log permeability measurements enable production rates prediction and allow optimization of production completion and programs stimulation while decreasing the cost of coring and testing wells especially in heterogeneous tight reservoirs where there is considerable permeability anisotropy [1].

This work focuses on determination of porosity ($\varphi_{DMR}$) from combination of density porosity and NMR porosity and permeability from NMR logs using Bulk Gas Magnetic Resonance Permeability (KBGMR), a technique proposed by Hamada et al. (2008) [2], and then using the neural network (NN) technique to predict formation porosity and permeability using NMR and conventional logging data. The NN technique has been developed and applied in several field cases and the predicted porosity and permeability values were validated from the proposed NN algorithm. Predicted porosity and permeability have shown a good correlation with core porosity and permeability in the studied gas sand reservoir.

## 2. Methodology

The field of interest is a gas condensate field producing from a Lower-Mesozoic reservoir. The reservoir is classified as a tight heterogeneous gas shaly sands reservoir. It suffers from lateral and vertical heterogeneity due to diagenesis effect (Kaolinite & Illite) and variation in grain size distribution. The petrophysical analysis indicates a narrow 8-12% porosity range, and a wide permeability range from 0.01 to 100 md. Figure 1 shows core porosity-permeability crossplot over whole reservoir section including all facies in different wells. It is obvious that this is a case of heterogeneous reservoir with six porosity- permeability zones of wide range. The core data shows cloud of points with undefined trend, which could be roughly subdivided into six or seven sub-regions [1, 3].

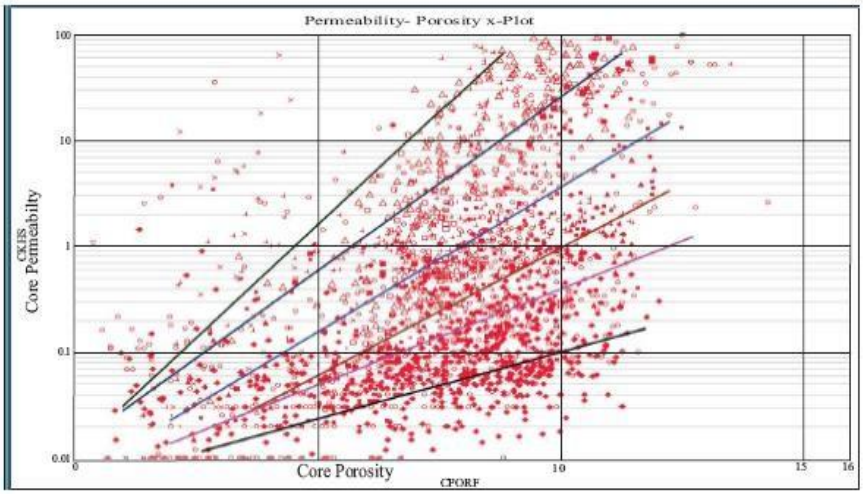


**Figure 1.** Porosity-permeability plot in heterogeneous gas sand [3]

In heterogeneous reservoirs, facies may change on few meters and down to few centimetres scales. The average fluid density in this case becomes unsatisfactory, this is mainly due to the heterogeneity of fluids distribution in the reservoir; thereupon, it is required to explore new porosity determination techniques that are independent of facies change. Due to reservoir heterogeneity; many cores were acquired in different wells covering different reservoir units to create the proper porosity-density and permeability models for each. The uncertainty associated with identification of the proper porosity and permeability model for each unit is high, which could result in high permeability estimation far beyond the actual well performance. Therefore, integration of non-standard tools like NMR with conventional

tools and special core analysis (SCAL) in the petrophysical evaluation is essential to reduce the uncertainty beyond the limitations of each tool in individual bases, especially in gas reservoirs [4-6].

## 3. Density-Magnetic Resonance Porosity ($\varphi_{DMR}$)

Freedman et al. (1998) proposed a combination of density porosity and NMR porosity ($\varphi_{DMR}$) to determine gas corrected formation porosity and flushed zone water saturation (Sxo) [7]. Density/NMR crossplot is superior to density/neutron crossplot for detecting and evaluating gas shaly sands. This superiority is because of thermal neutron absorbers in shaly sands on neutron porosities which causes neutron porosity readings to be shooting high. As a result, neutron/density logs can miss gas zones in shaly sands [3, 7]. On the other hand, NMR porosity readings are not affected by shale or rock mineralogy, and therefore density/ NMR (DMR) technique is the more reliable to indicate and evaluate gas shaly sands.

NMR porosity response in flushed gas zone is defined as

$$\varphi_{NMR} = \varphi S_{gxo} HI_g P_g + \varphi HI_L (1 - S_{gxo}) \quad (1)$$

Density porosity response in gas flushed zone is defined as

$$\rho b = \rho_m (1 - \varphi) + \rho_L \varphi (1 - S_{gxo}) + \rho_g \varphi S_{gxo} \quad (2)$$

Solution of Equations 1 & 2 for True Formation Porosity (Φ)

$$\varphi = A \times \varphi_D + B \times \varphi_{NMR} \quad (3)$$

where $HI_g$ & $HI_L$ are the hydrogen index in gas and liquid and $P_g$ is NMR gas polarization, $S_{gxo}$ is flush gas saturation and $\rho b$ is bulk density and A, B are factors.

### 3.1. Calibration for $\varphi_{DMR}$ Porosity:

A curve fitting method has been used to calibrate the A & B constants values which are applied to the reservoir of interest. In our case we have selected well (A) where both core and NMR data were available over the same reservoir interval. Assuming core porosities are equal to $\varphi_{DMR}$, which is the gas corrected porosity.

Equation 3 can be written in the following form.

$$\frac{\varphi_{Core}}{\varphi_{NMR}} = A \times \frac{\varphi_D}{\varphi_{NMR}} + B \quad (4)$$

The fitting trend line has a slope of A=0.65 and intercepts the Y axis at B=0.35, which results in DMR porosity transform as follows

$$\varphi_{DMR} = 0.65\varphi_D + 0.35\varphi_{NMR} \quad (5)$$

### 3.2. DMR Porosity Results

The results of $\varphi_{DMR}$ transform applications in the two test wells A & B showed very good match between $\varphi_{DMR}$ and core porosities as shown in Figures 2 and 3. As a result, it is considered being an independent facies porosity model. These corrected porosities can be used in conjunction with Timur-Coates equation [5] to estimate accurate permeability in gas bearing formations.

Figures 2 & 3 present well logs that show PHID & $\varphi_{DMR}$. Gamma ray and Caliper curves are shown in the first track (GR & CALI), second track shows depth in meters, the third one is resistivity, the fourth one is neutron-density logs, the fifth track shows comparison between core, density and NMR porosities,

the sixth track shows comparison between $\varphi_{DMR}$ and core porosity, the seventh track shows saturations of gas (green shadow) and water (blue shadow) and the last track shows core permeability in mD.

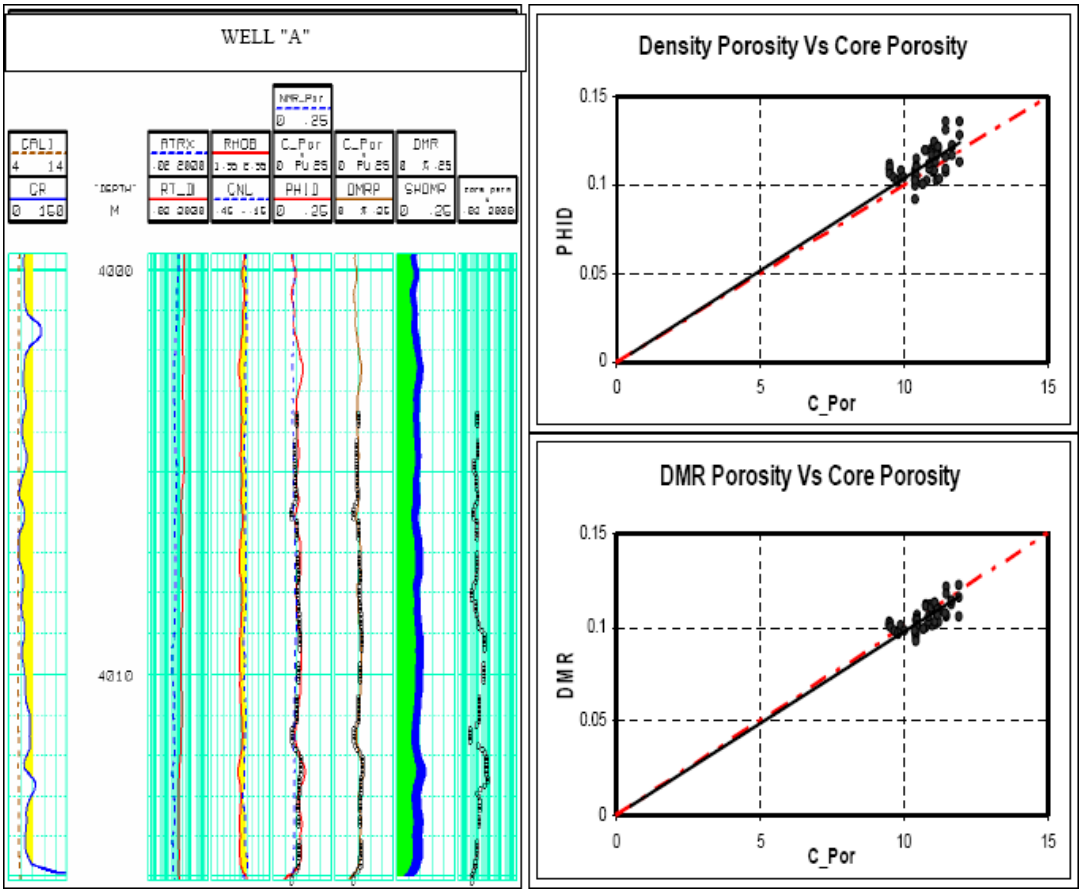


**Figure 2.** DMR Porosity and core porosity in well A [2]

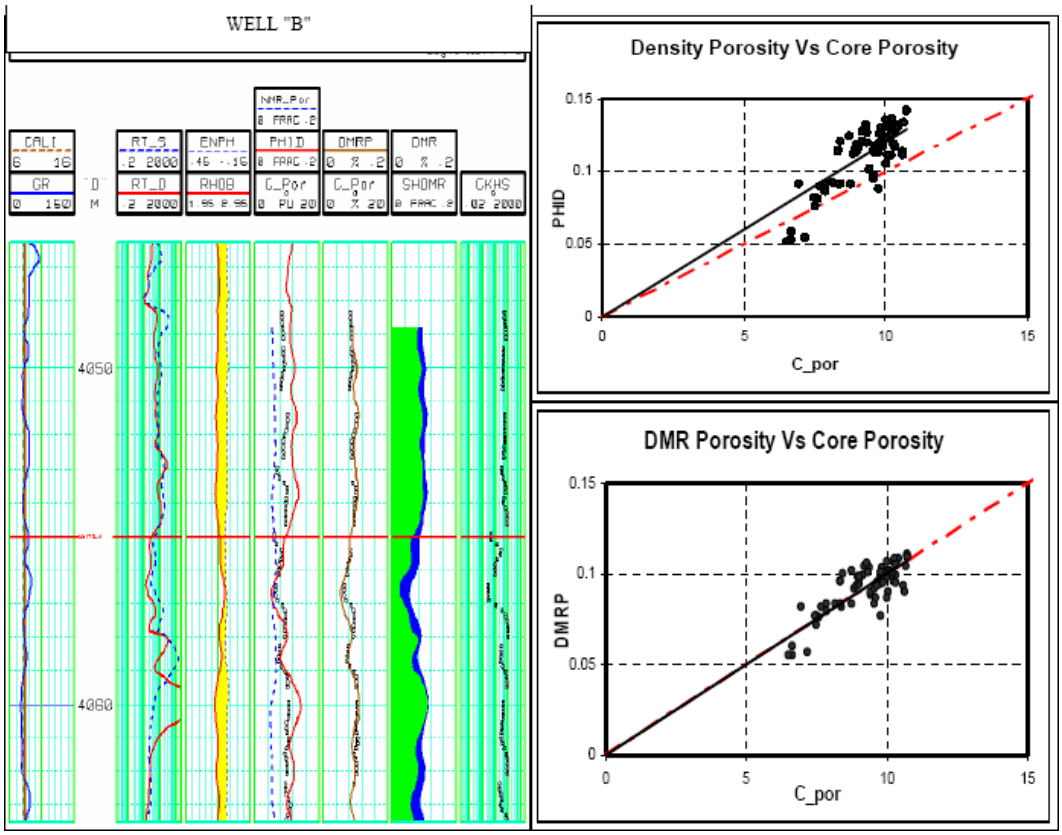


**Figure 3.** DMR Porosity and core porosity in well B [2]

The DMR method has the advantage of avoiding the use of fluid density and gas hydrogen index (HI) at reservoir condition for gas correction. Another advantage is that we can increase logging speeds as we do not need full polarization for gas [7, 8].

## 4. Gas Sand Permeability Estimation from NMR (KBGMR)

Bulk Gas Magnetic Resonance Permeability (KBGMR) technique is relatively new, presented by Abushanab et al. (2005) [3] for permeability estimation in gas reservoirs. It has the same value in oil-based mud (OBM) and water-based mud WBM conditions, as it depends on gas re-entry to the flushed zone after mud cake takes place and invasion stops. It is a dynamic concept of gas movement behind mud cake because of formation permeability, gas mobility and capillarity forces. Because gravity forces are constant, capillarity depends mainly on permeability and mobility depends on permeability and fluid viscosity which is constant for gas; the gas re-entry volume is a direct function on permeability.

### 4.1. BGMR Permeability Results

Permeability is derived from empirical relationship between NMR porosity and mean values of T2 relaxation times. Two permeability models are widely used in the industry Kenyon model [$K=cx(\varphi_{NMR})^a \times (T2)^b$] and Timer-Coates model [$K=[(\varphi_{NMR}/c)^a \times (BVM/BVI)^b$] [8]. Kenyon model permeability is affected by gas and OBM filtrate (non- wetting phase). Timer-Coates permeability model works well in gas reservoirs, but it is affected by uncertainty of bulk volume irreducible (BVI) cut off values and wettability alteration by oil base mud (OBM) filtrate. After defining T2 cut off values, it is time to calibrate the fitting parameters (a, b and c) for studied shaly gas sand reservoir. Permeability determination by Timer-Coates model in the case of tight heterogeneous shaly gas sand was not satisfactory because of rock facies, tightness and the significant variation of T2 values for the same facies. Estimates of Kenyon and Timer- Coates permeability are both affected by hydrocarbon; therefore,

the development of a different permeability model is essential. NMR derived permeability is based on bulk gas volume (BG) in flushed zone. It is the difference between DMR (density magnetic resonance) porosity and NMR porosity.

$$\text{BG volume} = \varphi_{DMR} - \varphi_{NMR} \quad (6)$$

The relationship can be normalized by dividing the gas volume by the total porosity of DMRP to be equal to flushed zone gas saturation, $S_{gxo}$

$$S_{gxo} = (\varphi_{DMR} - \varphi_{NMR})/\varphi_{DMR} \quad (7)$$

The correlation between Sgxo and permeability in md has the following form.

$$K_{BGMR} = 0.18 \times 10^{(6.4 \times S_{gxo})} \quad (8)$$

KBGMR formula has been applied into two wells A and B, where Figures 4 and 5 show the results of the two wells respectively. Wells A, B show a good match between KBGMR permeability with core permeability using the same KBGMR transform.

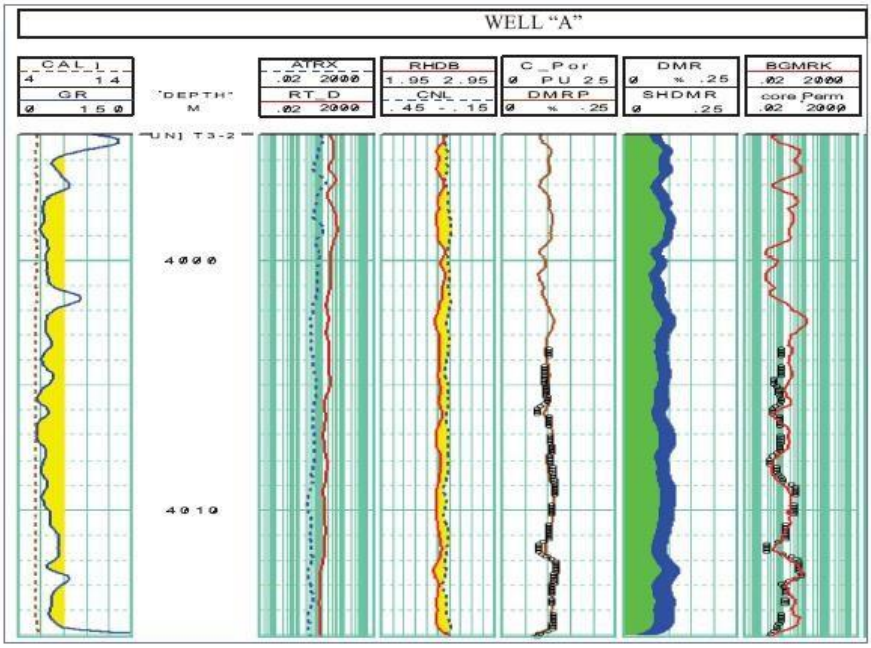


**Figure 4.** Well A, KBGMR permeability, track 6 [2]

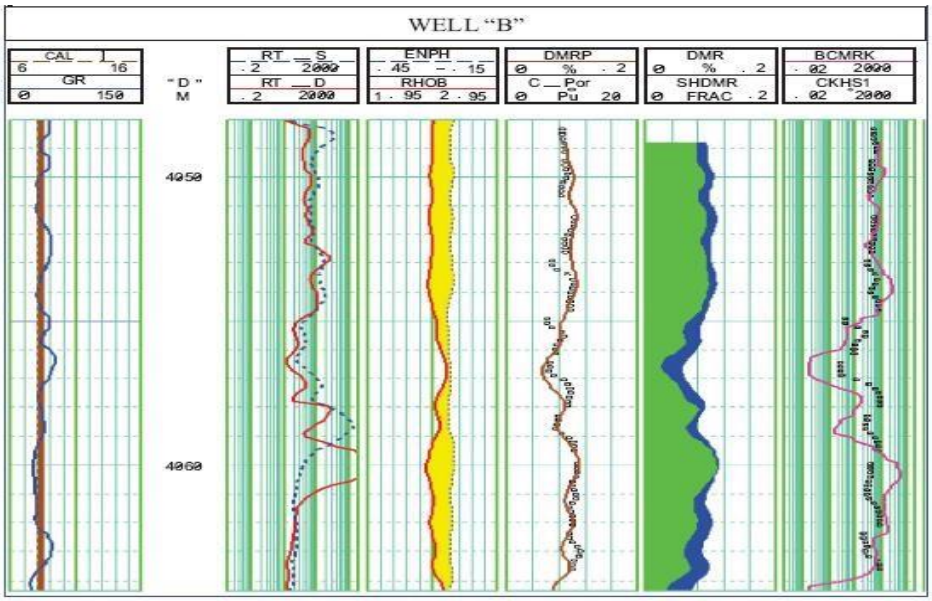


**Figure 5.** Well B, KBGMR permeability, track 6 [2]

## 5. Artificial Neural Network (ANN ) Interpretation of NMR Data

For obvious economic reasons, there has been a paradigm shift in hydrocarbon exploration and development strategies for better utilization of seismic data for reservoir characterization. Discovering the complicated and nonlinear relationship between seismic attributes and reservoir properties has been a major challenge for working geoscientists. Artificial Neural Network techniques have been proposed and proved to be effective in capturing these complex relations and have proven to be an effective modelling tool. Let $x_1$ , $x_2$ ,...., $x_p$ be the input signals, $w_{k1}$ , $w_{k2}$ ,...., $w_{kp}$ are synaptic weights of neuron k, $w_{k0}$ is a bias term, $v_k$ is the linear combiner output, f(.) is an activation function, and $y_k$ is the output signal of the neuron, the mathematical model of the k-th neuron is described as

$$V_k = \sum_{j=1}^{p} w_{kj} x_j + w_{k0} \qquad (9)$$

$$y_k = f(V_k)$$

The activation function, f (.), defines the output of a neuron in terms of the activity level at its input. There are several classes of artificial neural networks structures. The most common structure of ANN is known as multi-layer perceptron Feed Forward Neural Networks (FFNN). FFNNs are composed of layers of interconnected neurons. Usually, an input layer, a few hidden layers, and an output layer are used as shown in Figure 6. The input layer is essentially a direct link to the inputs of the first hidden layer. The output of each neuron may be connected to the inputs of all the neurons in the next layer. Signals are unidirectional i.e., they flow only from input to output [9].

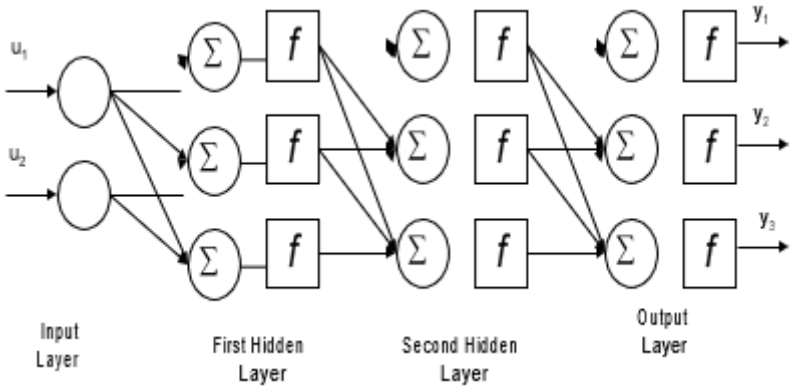


**Figure 6.** Multi-layer feed forward neural networks (FFNN)

The potential of FFNN as a basis for the modeling, classification, and statistical estimation stems from the following characteristics:

- For a sufficient number of hidden units, feed forward neural networks (FFNN) can approximate any continuous static input-output mapping to any desired degree of approximation [9, 10].
- Due to the modular and feed forward structure, the training of the network is simple and can be made to adapt to varying conditions.
- Number of neurons have selected and weighted within optimum level fitting to available data from conventional and NMR.

The back propagation (BP) algorithm is usually used for (FFNN) training [10]. Although BP is simple, the choice of a good learning rate requires some trial and error. Several improved variants of the BP algorithms were proposed in the literature, e.g., the RPROP algorithm, Riedmiller and Braun [11], Conjugate Gradient, Powell [12], and Levenberge- Marquardt (LM), Hagan and Menhaj [13]. Although all these algorithms suffer from sensitivity to the initial value of the weights and biases, the LM was shown to be the fastest algorithm for function approximation problems. The LM training algorithm is chosen for training the developed neural networks in this study [12, 14].

### 5.1. Porosity Prediction Using Artificial Neural Network (ANN)

Porosity is a key petrophysical parameter in formation evaluation. Consequently, new well logging techniques are developed to determine accurately formation porosity. Neural networks present an alternative approach to estimate porosity [12, 14-16]. Soto et al. (1997) developed a back propagation neural network with four layers to predict permeability and porosity from log data with satisfactory results [17]. Lim and Kim (2004) used artificial neural network to classify/identify lithofacies and predict permeability and porosity from well and they proposed the use of combined fuzzy logic artificial neural network to predict porosity and permeability [18]. Fuzzy curve analysis was used to select the best inputs for the artificial neural network from the available conventional well log data. Elshafei and Hamada (2007) estimated formation porosity and water saturation of shaly sand reservoirs with relatively satisfactory result using two separate neural network models from well logging measurements [19].

#### 5.1.1. ANN Porosity Prediction Using Conventional Log

The conventional log consists of 5 measurements: Gamma Ray (GR), bulk density (RHOB), Neutron porosity (CNL), Deep and shallow resistivity (RT_D, and RT_S). The NMR data consists of 10 T2 pin values. Data from two test wells A and B were combined and split to 60 % training and 40 % testing. A neural network consisting of 5 inputs, a single hidden layer of 16 neurons, and an output layer was built. The hidden layer consists of a tan-sigmoid function, and the output neuron is a log-sigmoid function.

The mean square root error during training (Figure 7) and testing (Figure 8) came to 0.0075 and 0.0102 respectively. The correlation between the predicted values and targeted values during training came to 0.912, and during testing 0.892. Figures 7 and 8 illustrates the correlation between predicted porosity and core porosity in cases of training and testing. These correlation coefficients are not very high, it may be attributed to the high noise level in the input data.

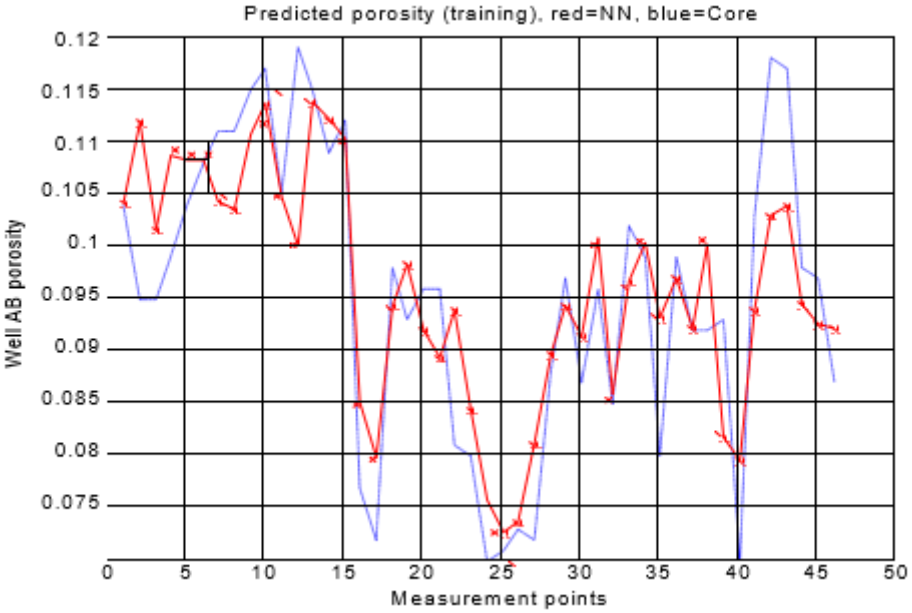


**Figure 7.** ANN prediction of porosity using conventional log, training performance

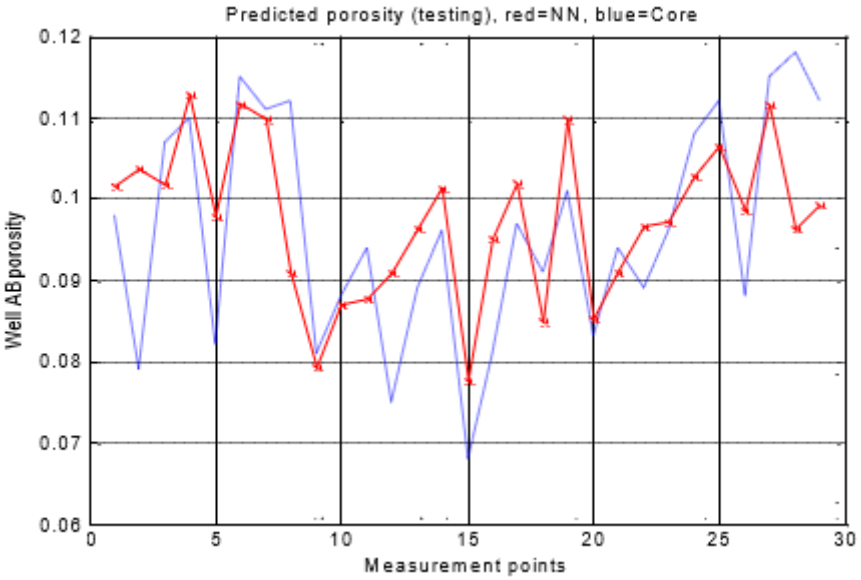


**Figure 8.** ANN prediction of porosity using conventional log, testing Performance

### 5.1.2. ANN Prediction of Porosity Using NMR and Conventional Log

The data used consists of 5 conventional logs, 10 T2 pins, and the mean value of the pins, the mean squared value of the pins, and the maximum value of the pins, a total of 18 parameters. Due to the richness of the data, a simple neural network provides an improved performance over the structure

used with the conventional log. The neural network consists of a single hidden layer of 8 neurons. The hidden neurons use tan- sigmoid function, and the output neuron uses a log-sigmoid function.

The root of the mean squared errors during training and testing came to 0.0038 and 0.0105 respectively (0.5). The correlation between the predicted values and targeted values during training (Figure 9) came to 0.9653 and during testing to 0.91 (Figure 10). The relatively poor performance is mainly due to the small number of core measurements (24 from well A, and 51 from well B, a total of only 75 scattered points).

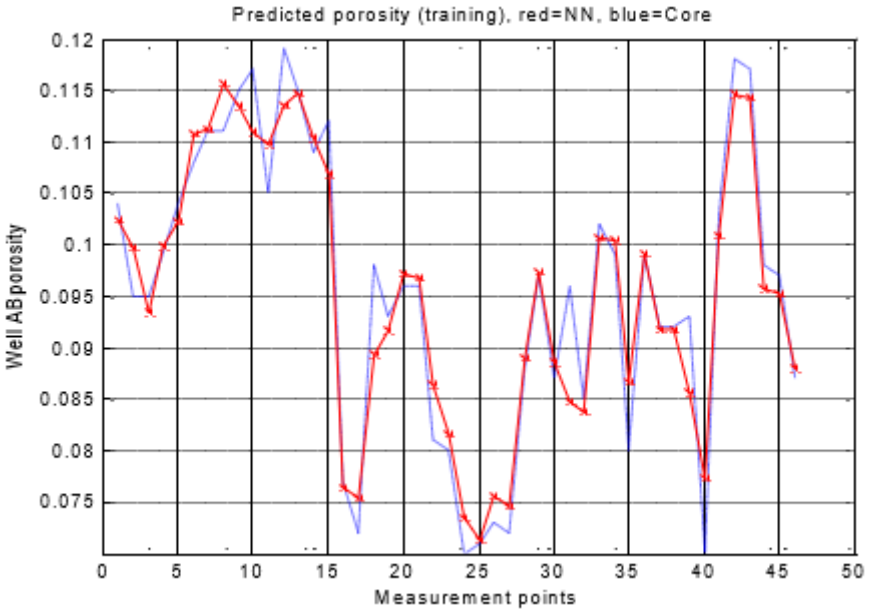


**Figure 9.** ANN prediction of porosity using conventional & NMR log, training performance

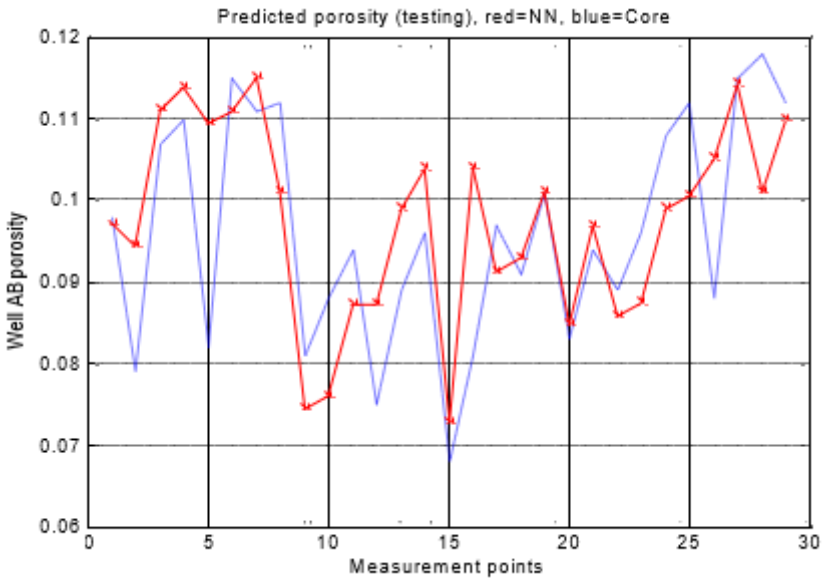


**Figure 10.** ANN prediction of porosity using conventional & NMR log, testing performance

## 5.2. Permeability Estimation Using Neural Network (ANN)

The determination of permeability characteristics is labor intensive and quite complicated. Empirical models to predict relative permeability from rock and fluid properties have also experienced relatively limited success. Hence alternative methodologies for accurate determination of relative

permeability characteristics have since been considered [13, 17-20]. Artificial neural network (ANN) approach is proposed to predict an accurate permeability. Balan et al. (1995) did comparative prediction of the permeability estimation from log data using empirical model, multiple variable regression, and artificial neural network [21]. The result shows that multiple regression and neural network techniques perform better than the empirical ones with neural network as cited as the best tool. Garrouch and Smaoni (1998) estimated tight gas sand permeability from porosity, mean pore size, and mineralogical data using a back-propagation neural network model with 8-input neuron and 2-5 hidden layers [15].

#### 5.2.1. Gas Sand Permeability Estimation from Neural Network (ANN)

Prediction of permeability by neural network (NN) approach needs good input logging data, such as NMR data (T2), in addition to conventional logging data (GR, density, Neutron, resistivity). The two wells A, B were analyzed to build a NN-based permeability prediction model.

#### 5.2.2. ANN Permeability Prediction Using Conventional Log

Conventional log data from wells A and B were combined and divided into two data sets, a training set of 60 % of data, and a test set of 40 % of data. It is preferred to start the prediction of permeability using conventional log alone, thereby using Figure 11 as a base line for later assessment of the NMR effectiveness.

The developed NN has five inputs and one hidden layer of 16 neurons. The hidden layer uses tan-sigmoid activation functions, and the output layer uses log-sigmoid activation function. All inputs were normalized between [-1, +1] based on the data available in wells A and B. The permeability was normalized on a log scale as $p_n=(\log_{10}(p_{true})+2)/5.0$. The performance of the developed NN on the training data is shown in Figure 11, and its performance on the test data is shown in Figure 12. The ANN achieves a root mean squared error of 6.8 (4.5% of the full-scale) during training, and 9.14 (6.09%) during testing, with correlation coefficient of R =0.975.

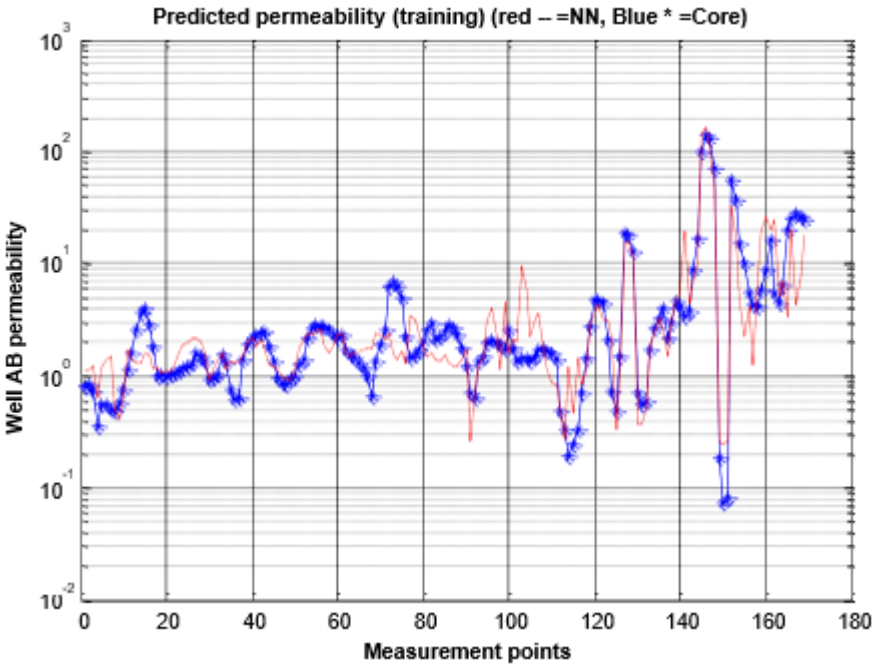


**Figure 11.** ANN prediction of permeability using conventional log, training performance.

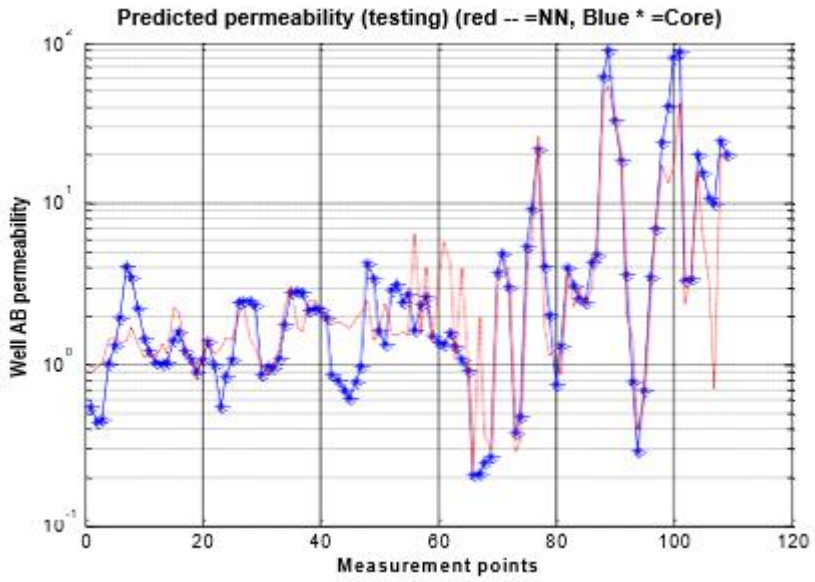


**Figure 12.** ANN prediction of permeability using conventional log, testing performance.

### 5.2.3. ANN Permeability Prediction Using NMR and Conventional Log

The data used consists of 5 conventional logs, 10 T2 pins, plus the mean value of the pins, the mean squared value of the pins, and the maximum value of the pins, making a total of 18 parameters. The conventional log data and the NMR data from wells A and B were combined and divided into two data sets, a training set of 60 % of data, and a testing set of 40% of data.

Due to the richness of the data, a simpler neural network provided an improved performance over the structure used with the conventional log. The neural network here consists of a single hidden layer of 8 neurons. The hidden neurons use tan-sigmoid function, and the output neuron uses a log-sigmoid function. Figure 13 shows the performance of the 18-input NN on the training data, and Figure 14 shows its performance on the test data. It is clear that there is excellent correlation between predicted permeability and NMR permeability curves.

The developed NN achieves a root mean squared error of 4.18 (about 2.8%) and of 4.515 (about 3.01%) on the training data and test data respectively. These results indicate that the NN manages to properly interpolate the test data and achieves almost uniform performance on the entire log data. The correlation coefficient came to R = 0.978 and 0.961 during training, and testing, respectively.

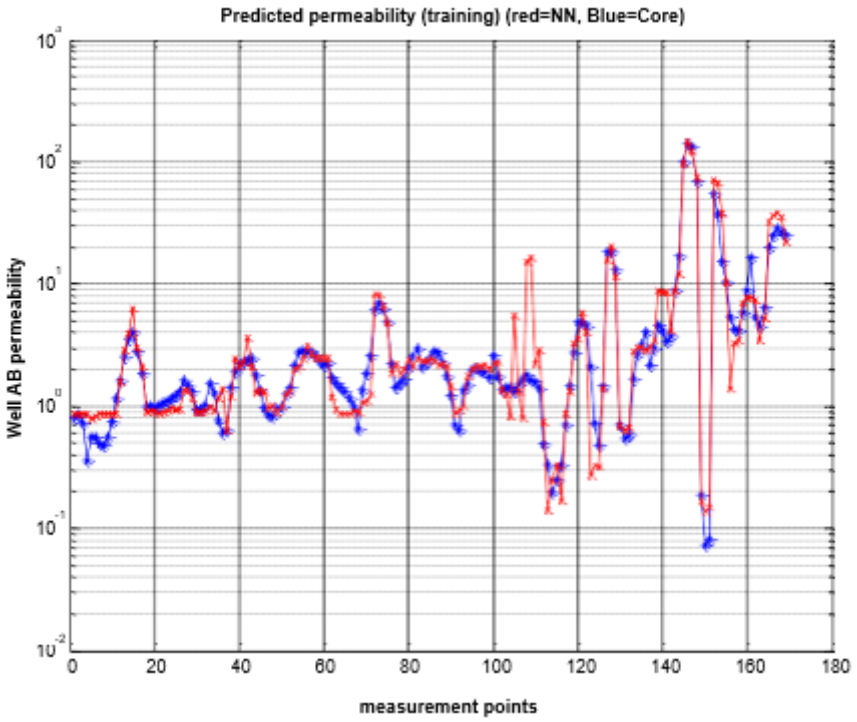


**Figure 13.** ANN prediction of permeability using conv. & NMR log, training performance.

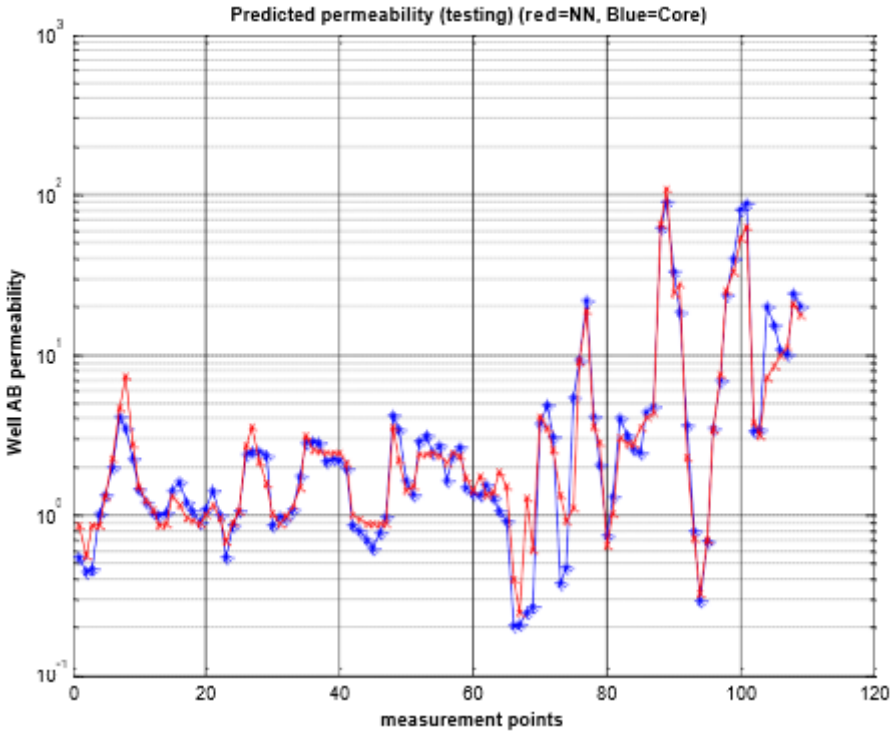


**Figure 14.** ANN prediction of permeability using conv. & NMR log, testing performance.

## 6. Conclusion

1. NMR derived permeability and, porosity have shown good matching with core tests results and BGMR permeability has shown excellent correlation with core permeability. DMR porosity iis recommend to be used rather than NMR or Density porosity separately

2. FFNN-predicted porosity using NMR and conventional log has an excellent matching with DMR NMR porosity in training and in testing sections that indicated an acceptable validation level of NN approach.

3. FFNN-predicted permeability from NMR decay times T2 and conventional logs has shown excellent matching with core permeability.

4. It is recommended to use the developed FFNN model to predict permeability from NMR data in other wells. It is also recommended to use combined artificial intelligence techniques (fuzzy, nonlinear algorithms and machine learning) in addition FFNN to get more accurate prediction of porosity and permeability of shay sandstone reservoirs.

**Nomenclature**

| | |
|---|---|
| φ | Porosity |
| Swi | Irreducible water saturation |
| Sgxo | Flushed zone gas saturation |
| FT | Formation tester |
| BVI | Bulk volume irreducible |
| OBM | Oil base mud |
| WBM | Water base mud |
| PHID | Density porosity reading |
| RT-D | True resistivity |
| RT-S | Flushed zone resistivity |
| NMR | Nuclear magnetic resonance |
| NN | Neural Network |
| BP | Back propagation training algorithm |
| KBGMR | Bulk Gas Magnetic Resonance Permeability |
| BG | Bulk gas volume |
| DMR | Density magnetic resonance |
| FFNN | Feed Forward Neural Network |
| LM | Levenberge-Marquardt training algorithm |

## References

[1] Oraby M., Habib E.-S., Negm E.: Experiences in Permeability Calculations in the Obayied Field (Egypt) Using Magnetic Resonance Imaging. in Middle East Oil Show and Conference. (1999 of Conference). DOI: 10.2118/53277-MS

[2] Hamada G. M., Shanab A., Oraby M. E.: New NMR approach evaluates tight gas sand reservoirs. Oil & gas journal, **106**, 46-53 (2008).

[3] Abu-Shanab M. M., Hamada G. M., El Oraby M.: DMR technique improves tight gas porosity estimate. Oil & gas journal, **103**, 54-54 (2005).

[4] Chardaire-Riviere C., Roussel J. C.: Principle and potential of nuclear magnetic resonance applied to the study of fluids in porous media. Revue de l'Institut français du pétrole, **47**, 503-523 (1992).

[5] Coates G. R., Menger S., Prammer M., Miller M.: Applying NMR Total and Effective Porosity to Formation Evaluation. in SPE Annual Technical Conference and Exhibition. (1997 of Conference). DOI: 10.2118/38736-MS

[6] Galarza T., Giordano S., Fontanarosa M., Saubidet M., Altunbay M., Saavedra B., Romero P.: Pore-Scale Characterization and Productivity Analysis by Integration of NMR and Openhole Logs–A Verification Study. in Latin American & Caribbean Petroleum Engineering Conference. (2007 of Conference). DOI: 10.2118/108068-MS

[7] Freedman R., Minh C. C., Gubelin G., Freeman J. J., McGinness T., Terry B., Rawlence D.: Combining Nmr And Density Logs For Petrophysical Analysis In Gas-Bearing Formations. in SPWLA 39th Annual Logging Symposium. (1998 of Conference).

[8] Kenyon B., Kleinberg R., Straley C., Gublin G., Morris C.: Nuclear magnetic resonance imaging-technology for 21st century, Autumn. (1995).

[9] Haykin S.: Neural Networks: A Comprehensive Foundation, MacMillan College Publishing Co. New York, (1994).

[10] Hornik K., Stinchcombe M., White H.: Multilayer feedforward networks are universal approximators. Neural Networks, **2**, 359-366 (1989). DOI: https://doi.org/10.1016/0893-6080(89)90020-8

[11] Riedmiller M., Braun H.: A Direct Adaptive Method for Faster Back propagation: The RPROP algorithm," presented at Proceeding of the IEEE International Conference on Neural Networks, USA (1993).

[12] Okon A. N., Adewole S. E., Uguma E. M.: Artificial neural network model for reservoir petrophysical properties: porosity, permeability and water saturation prediction. Modeling Earth Systems and Environment, **7**, 2373-2390 (2021). DOI: 10.1007/s40808-020-01012-4

[13] Hagan M. T., Menhaj M. B.: Training feedforward networks with the Marquardt algorithm. IEEE Transactions on Neural Networks, **5**, 989-993 (1994). DOI: 10.1109/72.329697

[14] Male F., Duncan I. J.: Lessons for machine learning from the analysis of porosity-permeability transforms for carbonate reservoirs. Journal of Petroleum Science and Engineering, **187**, 106825 (2020). DOI: https://doi.org/10.1016/j.petrol.2019.106825

[15] Garrouch A., Smaoui N. H.: An Artificial Neural Network Model for Estimating Tight Gas Sand Permeability. in SPE Asia Pacific Conference on Integrated Modelling for Asset Management. (1998 of Conference). DOI: 10.2118/39703-MS

[16] Maina A. I. h. M.: Caractérisation des réservoirs de pétrole/gaz à faible résistivité: Implication de la diagenèse pour une prédiction précise, prospect de Dibeilla, bassin de Termit, Niger. International Journal of Innovation and Applied Studies, 2028-9324 (2022).

[17] Soto B., Ferneynes E. L., Bejaramo H.: Neural network to predict the Permeability and porosity of zone C of the Cantagalo field. Colombia, Paper SPE, **38134**, (1997).

[18] Lim J.-S., Kim J.: Reservoir Porosity and Permeability Estimation from Well Logs Using Fuzzy Logic and Neural Networks. in SPE Asia Pacific Oil and Gas Conference and Exhibition. (2004 of Conference). DOI: 10.2118/88476-MS

[19] Elshafei M., Hamada G. M.: Neural Network Identification of Hydrocarbon Potential of Shaly Sand Reservoirs. in SPE Saudi Arabia Section Technical Symposium. (2007 of Conference). DOI: 10.2118/110959-MS

[20] Al-Bazzaz W. H., Al-Mehanna Y. W., Gupta A.: Permeability Modeling Using Neural-Network Approach for Complex Mauddud-Burgan Carbonate Reservoir. in SPE Middle East Oil and Gas Show and Conference. (2007 of Conference). DOI: 10.2118/105337-MS

[21] Balan B., Mohaghegh S., Ameri S.: State-Of-The-Art in Permeability Determination From Well Log Data: Part 1- A Comparative Study, Model Development. in SPE Eastern Regional Meeting. (1995 of Conference). DOI: 10.2118/30978-MS